

Review

Progress in Imidazolium Ionic Liquids Assisted Fabrication of Carbon Nanotube and Graphene Polymer Composites

Rengui Peng ^{1,†}, Yuanzhen Wang ^{1,†}, Wei Tang ¹, Yingkui Yang ^{1,*} and Xiaolin Xie ²

¹ Ministry-of-Education Key Laboratory for Green Preparation and Application of Functional Materials, Faculty of Materials Science and Engineering, Hubei University, Wuhan 430062, China

² School of Chemistry and Chemical Engineering, Huazhong University of Science and Technology, Wuhan 430074, China; E-Mail: xlxie@mail.hust.edu.cn

† These authors contributed equally to this review.

* Author to whom correspondence should be addressed; E-Mail: yingkuiyang@gmail.com; Tel.: +86-27-8866-1729; Fax: +86-27-8866-5610.

Received: 15 April 2013; in revised form: 31 May 2013 / Accepted: 4 June 2013 /

Published: 21 June 2013

Abstract: Carbon nanotubes (CNTs) and graphene sheets are the most promising fillers for polymer nanocomposites due to their superior mechanical, electrical, thermal optical and gas barrier properties, as well as high flame-retardant efficiency. The critical challenge, however, is how to uniformly disperse them into the polymer matrix to achieve a strong interface for good load transfer between the two. This problem is not new but more acute in CNTs and graphene, both because they are intrinsically insoluble and tend to aggregate into bundles and because their surfaces are atomically smooth. Over the past decade, imidazolium ionic liquids (Imi-ILs) have played a multifunctional role (e.g., as solvents, dispersants, stabilizers, compatibilizers, modifiers and additives) in the fabrication of polymer composites containing CNTs or graphene. In this review, we first summarize the liquid-phase exfoliation, stabilization, dispersion of CNTs and graphene in Imi-ILs, as well as the chemical and/or thermal reduction of graphene oxide to graphene with the aid of Imi-ILs. We then present a full survey of the literature on the Imi-ILs assisted fabrication of CNTs and graphene-based nanocomposites with a variety of polymers, including fluoropolymers, hydrocarbon polymers, polyacrylates, cellulose and polymeric ionic liquids. Finally, we give a future outlook in hopes of facilitating progress in this emerging area.

Keywords: carbon nanotubes; graphene; ionic liquids; polymers; nanocomposites

1. Introduction

Incorporation of nanosized fillers into polymers has created new composites by expanding the functions and applications while retaining the excellent manufacturing and processing flexibility inherent to polymers [1,2]. Polymer nanocomposites, therefore, have attracted substantial academic and industrial interest because of large commercial opportunities in the fields of automobile parts, coatings, flame retardants, and packaging, since their inception in the late 1980s. Nanoscopic particles appear to be a magic pixie dust that delivers huge dividends due to large property improvements of polymers at very small loading levels with respect to microscopic fillers. At present, various nanoparticles of 0D to 3D morphologies, such as layered clay, fumed silica, inorganic oxides, and carbon nanomaterials, have been applied to fabricate the composites with almost every engineering polymer [2,3]. Compared with traditional nanofillers, however, carbon nanotubes (CNTs) and more recently, graphene, have been increasingly recognized as the promising candidates for multifunctional components to strengthen and/or functionalize polymer nanocomposites [4–6].

Graphene is the first two-dimensional atomic crystal with one-atom-thick fabric of sp^2 -hybridized carbon atoms in a honeycomb crystal lattice [7]. It is also the thinnest known material available to us and is the mother of graphitic carbon materials [8]. CNTs are structurally constructed by rolling-up a single or multi graphene sheets into a seamless cylindrical tube, and hence they are classified into single-walled CNTs (SWCNTs) or multi-walled CNTs (MWCNTs) [9–11], respectively. Both theoretical and experimental results on graphene and CNTs show remarkable mechanical, electrical, thermal and optical properties [12–20]. The unique structure-dependent-properties have made CNTs and graphene greatly attractive for polymer composites in various applications including mechanically-reinforced materials [21–23], antistatic or conductive materials [24–26], biomaterials [27,28] as well as actuators [29–31], photonics [32] and solar cells [33–37] over the last three decades.

However, most of the above properties and applications are closely associated with isolated, individual CNTs and graphene. Unfortunately, CNTs intrinsically tend to form large clusters, bundles or ropes due to attractive van der Waals interactions between tubes coupled with high aspect ratio. Similarly, graphene is hardly soluble in general solvents, and have a strong tendency to agglomerate irreversibly or even to restack into graphite-like structures. For polymer nanocomposites, therefore, the critical challenges lie in fully, uniformly dispersing and exfoliating individual CNTs and graphene sheets into the polymer matrix to achieve strong interface that provides effective load transfer [2,4].

Many promising results have been achieved by the functionalization of CNTs and graphene in conjunction with the optimization of processing techniques of polymer composites [38–41]. Over the past years, we have found that MWCNTs functionalized by organic molecules [42,43], polystyrene (PS) [44,45], hyperbranched poly(urea-urethane) [46,47], biodegradable poly(ϵ -caprolactone) (PCL) [48,49], azobenzene-containing polyurethane [50] and ionic polymers [51] are well soluble in water or organic solvents. MWCNTs after functionalization can be uniformly dispersed and well bonded to the polymer matrix [52,53]. More recently, we have reported that liquid-like MWCNTs (*l*-MWCNTs) functionalized

by 2,2'-(ethylenedioxy)-diethylamine are individually integrated into the epoxy matrix by solvent-free processing, while solid MWCNTs functionalized by 1,8-diaminooctane and pristine MWCNTs produced poor dispersion and weak interface adhesion with the matrix under the same processing conditions [43]. The Young's modulus, storage modulus and tensile strength of neat epoxy are increased by 28.4%, 23.8%, and 22.9%, respectively, by adding 0.5 wt % of *l*-MWCNTs. The functionalized CNTs in liquid form contribute to better dispersion and superior interfacial bonding with the matrix, thereby facilitating greater mechanical reinforcement efficiency. The proposed methodology of using liquid-like CNTs provides a new way to process otherwise "solid fillers" to fabricate polymer composites.

Of special interest here is the fabrication of nanotube and graphene polymer composites assisted by imidazolium-based ionic liquids (Imi-ILs). ILs are generally defined as low-melting organic salts that are liquid below 100 °C while those with higher melting points are frequently referred to as molten salts [54]. Over the past decades, ILs has been frequently used as the eco-friendly, clean solvents and functional additives in the materials synthesis because of their "green" nature including negligible vapor pressure, incombustibility, high thermal stability, high product recovery and recycling ability in conjunction with tunable solubility and designable functionality [55–58]. Especially in 2003, Fukushima *et al.* [59] first found that the heavily entangled SWCNT bundles were well untangled in Imi-ILs after being ground. Afterwards, Tour *et al.* [60] have demonstrated that SWCNTs are effectively exfoliated and functionalized predominantly as individuals by grinding with aryl diazonium salts in the presence of ILs as green solvents. Recently, Han *et al.* [61] have reported that graphene sheets are stably dispersed in an Imi-IL of 1-butyl-3-methylimidazolium hexafluorophosphate (BmimPF₆) with the help of poly(1-vinyl-3-butylimidazolium chloride) [poly(VbimCl)]. More recently, we have shown that Imi-ILs functionalized graphene sheets are homogeneously embedded in the poly(methyl methacrylate) (PMMA) matrix and thus contribute to high electrical conductivity, low percolation threshold and large increases in storage modulus, glass transition temperature (T_g) and thermal stability compared to PMMA [62]. Over the past decade, the Imi-ILs assisted fabrication of polymer composites with CNTs and graphene has triggered an increasing attention [63]; however, a comprehensive review is still absent from the literatures. We herein aim to give a survey summary for recent progress about this emerging field.

2. Exfoliation of Carbon Nanotubes and Graphene Sheets in Imidazolium Ionic Liquids

2.1. Carbon Nanotubes in Imidazolium Ionic Liquids

CNTs are promising building blocks for high-performance composites that require homogeneous dispersion and exfoliation of CNTs to give individual tubes in the matrix phase. However, the as-received CNTs are produced in bundled form and are largely insoluble in both water and common organic solvents and hence, in the matrix. Over the past two decades, significant efforts have been devoted to finding appropriate solvents to directly disperse pristine CNTs. It has been reported that SWCNTs are stably dispersed in hexamethylphosphoramide, *N*-methylpyrrolidone (NMP), and *N,N*-dimethylformamide (DMF) which are featured by both high electron-pair donicity and low hydrogen-bonding parameters [64–66]. Dimethyl sulfoxide (DMSO), however, has been found to be a bad solvent for debundling of SWCNTs due to high electron-pair donicity alone [67]. In comparison

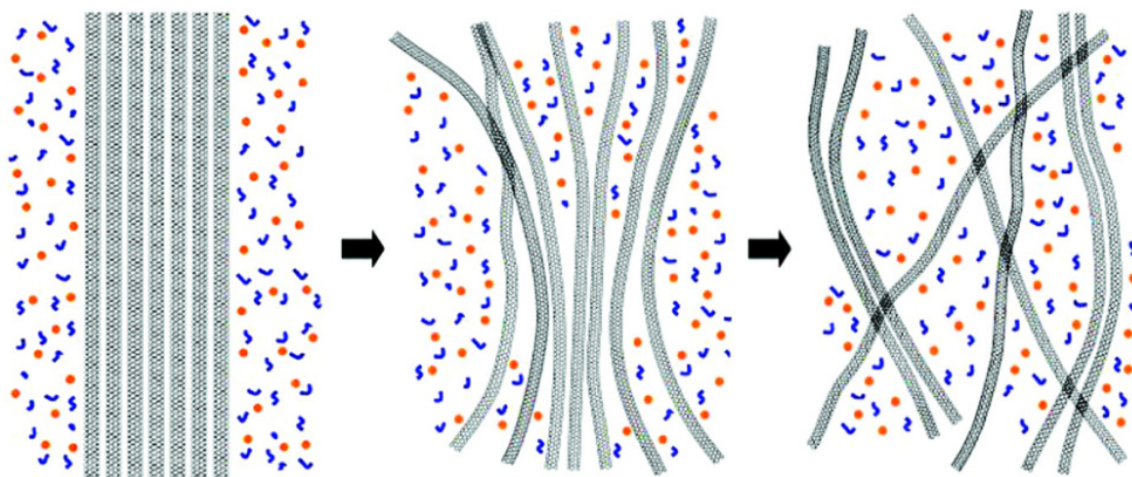
with DMF and NMP, an improvement in the dispersion limit of SWCNTs has been observed for alkyl amide solvents, such as *N,N*-dimethylacetamide (DMAc), *N,N*-dimethylpropanamide (DMP) and *N,N*-diethylacetamide (DEA), and is attributable to the highly polar π -system in conjunction with their optimal geometries (appropriate bond lengths and bond angles) [68]. In addition, chlorinated aromatic solvents, such as *mono*-chlorobenzene, *ortho*-dichlorobenzene (ODCB), *meta*-dichlorobenzene and 1,2,4-trichlorobenzene, have been demonstrated to be efficient at dispersing SWCNTs [69,70]. However, it has been found that phenyl rings within solvent molecules are not the dominant factor in obtaining stable SWCNTs dispersions [71]. This conclusion is reasonably proved by poor dispersibility of SWCNTs in toluene [67]. Therefore, the dispersion quality of CNTs closely depends on the choice of solvents. In studying the mechanisms of dispersion, Coleman *et al.* [72] have pointed out that good solvents for CNTs should be those with correct Hildebrand and Hansen solubility parameters based on cohesive energies and surface energies. It was predicted that successful solvents should possess surface tension close to $70 \text{ mJ}\cdot\text{m}^{-2}$ for matching between solvent and tube surface energy well [72]. The dispersion quality of CNTs in solvents is also affected by the nanotube concentration and processing techniques as well as the physical parameters of as-produced CNTs [68,69,71]. However, “stable suspensions” of SWCNTs in the best organic solvents (DMF and NMP) still aggregate on a time-scale of days, even minutes, in the absence of any external agents [64].

Over the past several decades, ILs, as potential green and designable solvents, have been widely used in the materials synthesis [54,58,73]. Fukushima *et al.* [59] first reported that SWCNTs and Imi-ILs were ground with an agate mortar to form a thermally stable gel (so-called “bucky gels”). The heavily entangled nanotube bundles were effectively exfoliated and disentangled into finer bundles even individuals within the gel (see Figure 2 in [59]). A “cation- π ” interaction between imidazolium ions of Imi-ILs and large π -electronic surface of SWCNTs is considered responsible for high debundling of nanotubes during grinding. Experimental data also provide the evidence for a cation- π interaction in the imidazolium-treated MWCNTs to account for this finding [74]. Furthermore, Shim and Kim [75] have studied the solvation of SWCNTs and MWCNTs in an Imi-IL of 1-ethyl-3-methylimidazolium tetrafluoroborate (EmimBF₄) using molecular dynamics simulations. They found that cations and anions of EmimBF₄ form the smeared-out cylindrical shell structures outside of nanotubes. Meanwhile, imidazole rings in the first internal and external solvation shells are mainly parallel to the nanotube surface to produce π -stacking, thus contributing to good dispersing capability.

However, experimental results in combination with the density functional theory calculations illustrate that there is no special (such as cation- π) interaction existing between CNTs and imidazolium ions [76]. In contrast, Imi-ILs interact with CNTs through weak van der Waals forces rather than the previous so-called “cation- π ” interaction. Molecular modeling studies further provide the evidence for this conclusion. A “ π - π ” interaction-shielding model is proposed to account for the dispersion process of CNTs in Imi-ILs as shown in Figure 1. Upon mechanically grinding CNTs with Imi-ILs, the nanotube bundles are gradually exfoliated by shearing force into smaller ones, and the detached tubes are immediately surrounded by Imi-ILs. The strong π - π stacking among CNTs is effectively shielded by Imi-ILs due to large dielectric constants of the latter and hence, preventing the disentangled bundles from rebundling. Meanwhile, the high surface energy of the isolated CNTs can be appeased since they are encapsulated by Imi-ILs through van der Waals forces. This implies that the shielding effect of Imi-ILs on the π - π stacking interaction among CNTs plays the key role in dispersing CNTs.

Although the dispersion mechanism of CNTs in Imi-ILs seems to be still a little controversial, Imi-ILs can disperse CNTs more efficiently than common solvents and stabilize them for a long time. For instance, it is difficult to directly disperse pristine CNTs in an aqueous solution. However, stable homogeneous suspensions can be obtained by dispersing pristine SWCNTs in water in the presence of 1-hexadecyl-3-vinylimidazolium bromide (HvimBr) above its critical micelle concentration [77]. The suspension concentrations of SWCNTs promoted by HvimBr are increased by at least 20% with respect to commonly used surfactants, such as sodium dodecyl sulfate, sodium dodecyl benzene sulfonate and cetyl trimethyl ammonium bromide. Moreover, it has been found that SWCNTs bundles are simultaneously exfoliated and chemically functionalized predominantly as individuals by grinding them with aryl diazonium salts in Imi-ILs [60]. This reaction occurs in minutes at room temperature, and is an extremely rapid and mild green protocol to exfoliate and functionalize SWCNTs. Imi-ILs have been successfully used as green media for the functionalization of SWCNTs and MWCNTs with various polymers, such as PCL [49], poly(*N*-succinimidyl acrylate) [78], poly(methylpyrrole) [79] and polyaniline [80]. All functionalized-CNTs show much better solubility and stability than pristine ones in solvents. In addition, the use of Imi-ILs as reaction media can enhance the reaction rate and grafting amount of polymer compared to conventional solvents [49]. More importantly, the production of stable homogeneous suspensions of CNTs in Imi-ILs without external dispersants emerges as a powerful strategy toward fabricating polymer composites.

Figure 1. Schematic of the dispersion process for carbon nanotubes (CNTs) in Imi-ILs. Reproduced with permission from [76]. Copyright 2008 the American Chemical Society.



2.2. Graphene Sheets in Imidazolium Ionic Liquids

CNTs can be structurally viewed as rolled-up graphene sheets seamlessly and hence, they both have similar conjugated structures and physicochemical features. These solvents mentioned in Section 2.1 should be applied to disperse and exfoliate graphene sheets. Till now, the solution-phase isolation of graphene has been carried out by two different categories [81]. The most commonly used strategy involves the strong acidic oxidation of graphite followed by exfoliation, producing graphene oxide (GO) platelets. GO can be then reduced by chemical, thermal and optical methods that restore partially sp^2 hybridization to yield reduced graphene oxide (RGO) [82,83]. RGO sheets thus retain some structural

and chemical defects, and are stable in DMF [84–86], NMP [85,87,88], DMAc [89] and propylene carbonate [90] with the concentration of up to $1.4 \text{ mg}\cdot\text{mL}^{-1}$. The second methodology is to directly exfoliate graphite into less defective (or defect-free) single- or few-layer graphene sheets in suitable solvents by means of ultrasonic energy, microwave irradiation or other techniques. It has been reported that the solvent-exfoliated graphene dispersions can be produced by direct exfoliation of graphite in organic solvents such as DMF [86,91,92], NMP [93,94], ODCB [95] and surfactant/water solutions [96] or supercritical fluids [97]. However, the maximum concentration of graphene sheets achieved is still low ($<1 \text{ mg}\cdot\text{mL}^{-1}$) and can only increase to $2 \text{ mg}\cdot\text{mL}^{-1}$ by a low-power sonication regime over long time frames (460 h) [94].

By analogy to CNTs, graphene should have surface energy close to that of Imi-ILs which would be promising solvents for the exfoliation of graphite into graphene [81,98]. Luo *et al.* [99] first presented a one-step electrochemical approach for the exfoliation of anode graphite rod to graphene sheets with the aid of Imi-ILs and water. Later, Loh *et al.* [100] reported a similar method to generate graphene using electrochemical exfoliation of the graphite anode in an aqueous electrolyte containing BmimBF₄ or 1-butyl-3-methylimidazolium chloride (BmimCl). In contrast, Dai *et al.* [101] employed ultrasonic energy to directly exfoliate graphite flakes in an Imi-IL of 1-butyl-3-methylimidazolium bis(trifluoromethanesulfonyl)imide (BmimTf₂N) followed by high-speed centrifugation to remove the fast sedimenting graphite. The supernatant suspension contains graphene sheets in BmimTf₂N has a concentration of up to $0.95 \text{ mg}\cdot\text{mL}^{-1}$ and exhibits the Tyndall effect of its diluted suspension (see Figure 1 in [101]). Most graphene sheets consist of less than five atomic layers with several micrometre-long edges. Mariani *et al.* [102] reported an improved protocol in which graphite flakes were ground with an Imi-IL of 1-hexyl-3-methylimidazolium hexafluorophosphate (HmimPF₆) in a mortar before sonication. Lateral sizes of graphene sheets are on the order of several micrometres with an average thickness of *ca.* 2 nm, corresponding to 6–7 layers. This simple method allows producing a graphene concentration as high as $5.33 \text{ mg}\cdot\text{mL}^{-1}$. Bulk quantities of graphene sheets with 2–5 layers thick have also been produced by mechanical grinding exfoliation of natural graphite in BmimPF₆ [103]. It is suggested that Imi-ILs assisted exfoliation of graphite and subsequent stabilization of graphene are attributable to the π - π and/or cation- π interactions between graphene and imidazole ions as well as strong charge polarization of graphene by Imi-ILs [101].

Safavi *et al.* [104] have recently proposed a new route for mass production of graphene by thermal treatment of graphite/ionic liquid crystal (ILC) composites. In their work, the ILC of 1,1'-didodecyl-4,4'-bipyridinium bis(triflimide) was mixed with graphite powder by hand-mixing in a mortar. Successive mixing and heating (up to 100 °C) of the mixture formed a uniform graphite/ILC composite, which was then heated at 700 °C for 1 h in a furnace under argon protection. Intercalation of ILCs between graphite layers followed by their decomposition and evolution of gases assisted in the exfoliation of graphite and separation of layers. The as-synthesized graphene sheets have lateral sizes of a few micrometers and 82% of them comprise 2–10 layers. The present method enables the facile, fast exfoliation of graphite to produce high-quality graphene in large quantities.

There are only a few reports about the IL-assisted direct exfoliation of graphite to graphene sheets. However, Imi-ILs have been frequently used during reduction of GO, and play a multifunctional role in the dispersion, stabilization, functionalization and hybridization of RGO sheets [105]. Han *et al.* [61] successfully obtained a stable suspension of RGO in hydrophobic BmimPF₆ by chemical reduction

of GO with hydrazine monohydrate in the presence of poly(VbimCl). Zhang *et al.* [106] also prepared stable dispersions of RGO in hydrophilic ILs including BmimBF₄, *N*-butylpyridinium tetrafluoroborate (BpyBF₄) and 1-allyl-3-methylimidazolium chloride (AmimCl) without using surfactants/stabilizers. The suspension concentration of RGO is up to 7.0 mg·mL⁻¹ which should be the highest value reported so far. Ji *et al.* [107] fabricated Imi-IL/RGO films by chemical reduction of GO in the presence of Imi-ILs at room temperature and the subsequent layer-by-layer assembly. They further reported the use of layered Imi-IL/RGO films on quartz crystal microbalances for selective gas sensing and found that the nanospace between graphene sheets has a higher affinity for toxic aromatic hydrocarbons than for their aliphatic analogues. The Imi-IL/RGO composite electrodes were also successfully used for the highly sensitive detection of trinitrotoluene [108,109], nitric oxide [110], chlorophenols [111], glucose [112], azithromycin [113], and hydroquinone and catechol [114].

ILs consist entirely of ions with high polarity and can produce highly efficient microwave absorption and hence, triggering rapid dielectric-heating through an ionic conduction mechanism. Yoon *et al.* [115] reported a facile method for thermal reduction of GO within 15 s by microwave irradiation in 1-ethyl-3-methylimidazolium bis(trifluoromethylsulfonyl)amide (EmimTf₂N). The as-fabricated supercapacitor by RGO operating at 3.5 V, shows high energy density (~58 W·h·kg⁻¹) and high power density (~246 kW·kg⁻¹). Small ruthenium and rhodium nanoparticles can be uniformly supported on RGO by microwave irradiation of metal carbonyl precursors in BmimBF₄ [116]. The resulting nanohybrids can be effectively used as catalysts for the hydrogenation of cyclohexene and benzene under solvent-free conditions. Ye *et al.* [117] found that RGO sheets could be obtained by one-pot hydrothermal reduction of GO in an Imi-IL in the presence of ascorbic acid, with concomitant growth of TiO₂ nanoparticles on the RGO surface. Similarly, Ag nanoparticles can be grown on the RGO surface by one-pot hydrothermal reduction of GO and silver nitrate in a suspension of BmimPF₆ and water [118]. Recently, Ag/RGO hybrids have been fabricated by gamma radiation-induced simultaneous reduction of GO and silver ions in water with the aid of EmimAc at room temperature [119]. The Raman signals of RGO are greatly enhanced by the attached Ag nanoparticles, showing surface-enhanced Raman scattering activity [118,119]. Besides, Kuang *et al.* [120] found that GO and Au (I) could be electrochemically co-reduced in BmimPF₆ to yield Au/graphene composites, showing great electrochemical catalytic activity and stability.

Moreover, immobilization of ILs on the solid supports can combine the advantages of ILs with those of heterogeneous supports. For instance, an amine-terminated Imi-IL, 1-(3-aminopropyl)-3-methylimidazolium bromide (ApmimBr), was grafted to the surface of RGO which thus could be dispersed in water, DMF and DMSO due to the enhanced solubility and electrostatic inter-sheet repulsion by Imi-IL units [121]. The ApmimBr-grafted RGO can be used to not only fabricate the biosensor for the electrochemical determination of β -nicotinamide adenine dinucleotide (NADH) and ethanol [122], but also produce new composites containing Pt nanoparticles with high electrocatalytic activity toward oxygen reduction [123].

3. Imidazolium Ionic Liquids Assisted Fabrication of Polymer Composites

3.1. Fluoropolymer Composites

3.1.1. With Carbon Nanotubes

Nafion is the first fluoropolymer used for the CNT composites [124], and the resulting composite film behaves as potential electrochemical actuators in an aqueous lithium chloride solution, showing tip deflections up to 4.5 mm at a voltage excitation of ± 2 V (1 Hz). Aida *et al.* [125] reported a fully plastic actuator that adopts a bimorph configuration with a fluoropolymer-supported internal electrolyte layer sandwiched by two electrode layers of fluoropolymer-based bucky-gel of Imi-ILs and SWCNTs. The latter was readily fabricated by grinding SWCNTs (13 wt %) in BmimBF₄ (54 wt %) for minutes with an agate mortar, followed by transferring to a mixture of poly(vinylidene fluoride-*co*-hexafluoropropylene) (PVDF-HFP, 33 wt %) and 4-methyl-2-pentanone. The heavily entangled SWCNTs are exfoliated in BmimBF₄ to form much finer bundles in the PVDF-HFP matrix. The bucky-gel actuator operates quickly in air in response to low electric potentials; for instance, the displacement of actuator strip was increased from 0.36 to 1.8 mm, as the applied voltage was changed from ± 1.0 to ± 3.0 V (0.1 Hz), respectively. The bending motion can be repeated in air for more than 8000 cycles without a notable decay. They also used a ball-milling method to prepare the casting suspension for the bucky-gel electrodes, and fabricated the actuators by hot-pressing the electrolyte film sandwiched by two electrode films [126]. Of note, the actuated properties of solid-state actuators are closely related to the Imi-IL species used [127,128]. Similar plastic actuators can be fabricated by using the activated carbon nanofibers instead of CNTs [129]. Such plastic actuators allow quick and long-lived operation at a low voltage in air. The present methods are easy process for the fabrication of plastic actuators and provide an important step toward developing the low-voltage driven solid-state devices.

By using a similar process, Aida *et al.* [130] uniformly dispersed millimeter-long SWCNTs into the PVDF-HFP matrix with the help of BmimTf₂N. The resulting SWCNT composite film was then coated by polydimethylsiloxane (PDMS) to obtain an elastic conductor with a conductivity of 5700 S·m⁻¹ and a stretchability of 134%. The elastic conductor was further integrated with printed organic transistors to fabricate a rubberlike-stretchable active sheet that can be uniaxially and biaxially stretched by 70%. Later, they fabricated a printable elastic conductor comprising SWCNTs uniformly dispersed in the vinylidene fluoride-tetrafluoroethylene-hexafluoropropylene copolymer [131]. A stretchable active-matrix display was then constructed by integrating printed elastic conductors and organic transistors with organic light-emitting diodes, and it could be stretched by 30%–50% and spread over a hemisphere. Such elastic conductors allow for the construction of large-area electronic integrated circuits especially mounted on the arbitrary curved surfaces and movable parts [132].

Recently, Mandal *et al.* [133] have reported that covalently functionalized MWCNTs by an Imi-IL of 3-aminoethyl imidazolium bromide can be uniformly dispersing in the PVDF matrix by solution casting or melt-blending. The PVDF composites show a very low percolation threshold (0.05 wt %) and a large increase in the conductivity due to the improved dispersion and interface in the presence of the anchored Imi-ILs.

3.1.2. With Graphene

In a recent work reported by Pandey *et al.* [134], a graphene-based all-solid-state supercapacitor was successfully fabricated by a gel electrolyte consisting of BmimBF₄ and PVDF-HFP. Cyclic voltammetry studies show that the supercapacitor has a capacitance of 80 mF·cm⁻², which is equivalent to single electrode specific capacitance of 76 F·g⁻¹. This corresponds to specific energy of 7.4 Wh·kg⁻¹ and specific power of 4.5 kW·kg⁻¹, respectively. Furthermore, the supercapacitor cell shows stable cyclic performances for up to 5000 cycles.

3.2. Hydrocarbon Polymer Composites

3.2.1. With Carbon Nanotubes

Hydrocarbon polymers, such as PS, polypropylene (PP), and polyethylene (PE), are hydrophobic in nature similar to fluoropolymers. CNTs may be viewed as all-carbon macromolecules, which are also hydrophobic intrinsically. Even PS has aromatic rings on its side-chain and may interact with the π -conjugated surface of CNTs, however, it is near impossible to produce the homogeneous composites by directly mixing pristine CNTs with hydrocarbon polymers [135]. Gilman *et al.* [74] successfully functionalized MWCNTs with 1,2-dimethyl-3-hexadecylimidazolium tetrafluoroborate (DhimBF₄) by melt blending at 185 °C in a twin-crew mini-extruder. The processing temperature is higher than the liquid-crystalline transition temperature (clearing point at 175 °C) of DhimBF₄. After cooling, DhimBF₄-modified MWCNTs were ground into powders and were then added to the PS matrix at 195 °C. It was found that unmodified-MWCNTs were hardly dispersed and appeared as large bundles while DhimBF₄-modified MWCNTs were uniformly, even individually exfoliated into the PS matrix (see Figure 1 in [74]). Therefore, DhimBF₄ acts as a compatibilizer to improve the affinity of MWCNTs for PS and hence, preventing re-aggregation of nanotubes in the PS matrix.

In the work of Wei *et al.* [136], SWCNTs were ground with BmimPF₆ and PS beads were added to the bucky-gel and then ground to produce a composite gel. It was found that SWCNTs were well embedded inside BmimPF₆ and, after being ground with PS, also dispersed in the BmimPF₆-PS matrix. The composite gel was sandwiched between a bottom ITO glass and a top Al electrode to construct a memory device. By tuning the concentration of SWCNTs, the electrical properties of the device vary from an insulator, a memory in terms of switching or negative differential resistance to a conductor. Recently, Bermúdez *et al.* [137] mixed SWCNTs with 1-octyl-3-methylimidazolium tetrafluoroborate (OmimBF₄) in an agate mortar and sonicated the mixture to obtain OmimBF₄-functionalized SWCNTs. To the PS matrix was added 1 wt % of functionalized-SWCNTs, and the composite obtained by milling was compression moulded for the measurement of tribological properties. It was found that the wear rate significantly decreases by 74% for the PS composite in comparison with neat PS due to the presence of well-dispersed SWCNTs bridging the gap through the crack opening.

3.2.2. With Graphene

Graphite exists abundantly in nature and thus is inexpensive and available in large quantities; however, it is not easy to readily exfoliate bulk graphite into individual graphene sheets. Luo *et al.* [99]

reported the facile preparation of graphene via the Imi-ILs assisted electrochemical functionalization of graphite. Four Imi-ILs were used including BmimPF₆, OmimBF₄, 1-octyl-3-methylimidazolium chloride (OmimCl), and 1-octyl-3-methylimidazolium hexafluorophosphate (OmimPF₆). The Imi-IL functionalized graphene sheets were well dispersed into polar solvents such as DMF for weeks. Graphene/PS composites were then prepared by solution mixing in DMF and their electrical conductivities were also measured. A percolation threshold of 0.1 vol % is observed for the OmimPF₆-functionalized graphene/PS composite with a conductivity of up to 13.84 S·m⁻¹ at 4.19 vol % loading. The percolation transition appears at *ca.* 0.13 and 0.37 vol % for the PS composites with graphene functionalized by OmimBF₄ and BmimPF₆, respectively, and their highest conductivities are *ca.* 6.59 and 3.61 S·m⁻¹, respectively. However, the PS composite with graphene obtained in the presence of OmimCl has no conductivity because of graphene oxidation by Cl₂ or O₂ produced on the anode. This indicates that Imi-ILs play an important role for the final properties of graphene/polymer composites during processing.

3.3. Polyacrylate Composites

3.3.1. With Carbon Nanotubes

In the work presented by Bermúdez *et al.* [137], OmimBF₄-functionalized SWCNTs (1 wt %) were also mixed with PMMA by milling to afford the composites. The dry tribological performance was studied against AISI 316L stainless steel pins and compared with that of neat PMMA and pristine SWCNT/PMMA composite without OmimBF₄. A significant decrease in the wear rate was observed for the functionalized-SWCNT/PMMA composite, which shows reductions of 63% and 58% with respect to PMMA and SWCNT/PMMA composite, respectively. This is attributable to the presence of OmimBF₄ which improves the lubricating ability and enables good dispersion of SWCNTs preventing the crack propagation and fracture. However, the wear rate was only reduced by 14% for neat polycarbonate (PC) when 1 wt % of SWCNTs were added by the same processing procedure. The less uniform dispersion of SWCNTs in PC should be responsible for its poorer wear performance possibly due to the worse compatibility between PC and the OmimBF₄ stacked on SWCNTs.

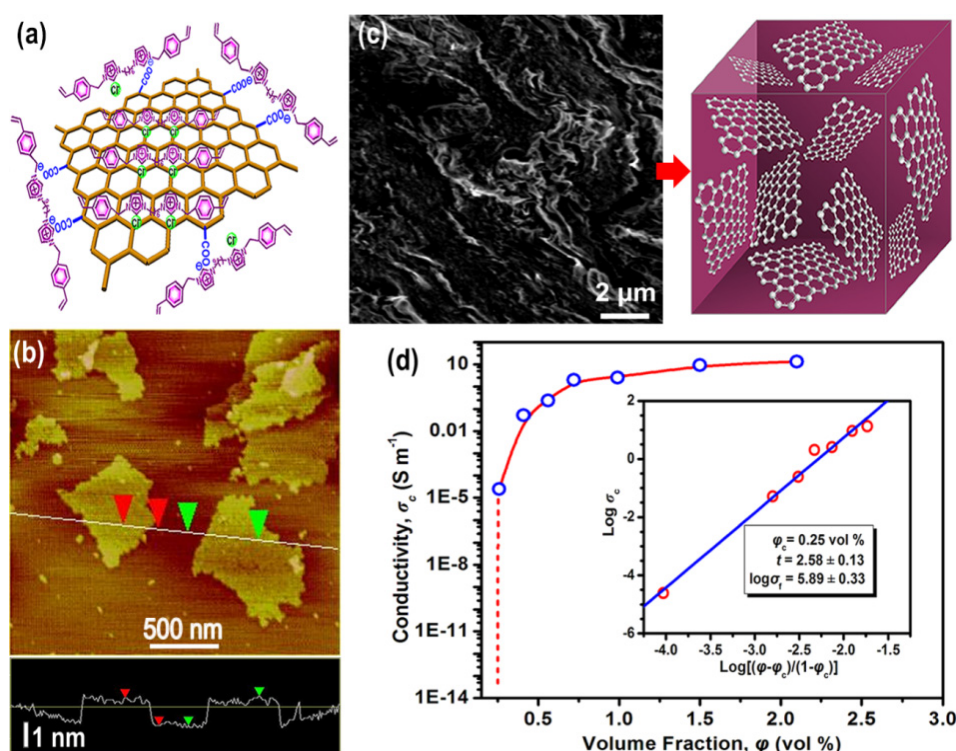
Recently, Li *et al.* [138] fabricated MWCNT/PMMA composites by melt-mixing of PMMA with MWCNTs in a batch mixer with a twin screw in the presence of BmimPF₆. There are mainly large agglomerates of MWCNTs in the composite without BmimPF₆, while the MWCNT agglomeration decreases significantly to 10–100 nm plus many individual nanotubes when a few amount of BmimPF₆ was used during processing (see Figure 2 in [138]). However, a further increase in the ratio of BmimPF₆ to MWCNTs produces almost individually dispersed tubes throughout the PMMA matrix. Moreover, BmimPF₆ plays a role of a plasticizer, inducing a drastically reduced *T_g* of PMMA. The proposed method via solvent-free processing is compatible with industrial applications, and provides a new way for the fabrication of CNT/polymer composites on a large scale.

3.3.2. With Graphene

Using RGO nanosheets as fillers has been the predominant methodology for the fabrication of graphene polymer composites. However, bulk graphene sheets from RGO tend to restack as a graphite-like structure and show low dispersion in various solvents and polymers. Recently, we have reported a

novel method to fabricate graphene/PMMA composites [62]. Initially, the functionalized graphene sheets were produced by chemical reduction of GO with NaBH_4 in the presence of NaOH and 1,6-bis[3-(vinyl benzyl)imidazolium-1-yl]hexane chloride (VbimBr) (Figure 2a). It was found that VbimBr could be non-covalently stacked on the large π -conjugated basal plane of graphene via π - π and/or cation- π interactions with imidazole rings (Figure 2b). Meanwhile, NaOH interacted with the residual carboxyl groups at the edges of RGO to form negatively charged graphene, which was found to further undergo an ion-exchange with the positively charged imidazolium groups of VbimBr. This process not only allows restoration of the π -conjugated graphene lattice and retains its electronic property, but also makes full use of the residual carboxyl groups of RGO. Finally, vinyl benzyl groups on the surface of VbimBr-functionalized graphene sheets could act as cross-linking reactive sites to *in situ* copolymerize with MMA monomer, producing graphene/PMMA composites. As expected, graphene sheets were uniformly dispersed in the matrix with a strong interface (Figure 2c) and thus contributed to large increases in storage modulus (+58.3%) and T_g (+19.2 °C) at 2.08 vol % loading. High electrical conductivity was also achieved at graphene loading levels beyond 1 vol % ($2.55 \text{ S}\cdot\text{m}^{-1}$) with a low percolation threshold (0.25 vol %) for the composites (Figure 2d). This work develops a general method to prepare graphene-based composites with vinyl polymers.

Figure 2. (a) Structural illustration for VbimBr-functionalized graphene; (b) AFM image of VbimBr-functionalized graphene sheets on a mica substrate and its corresponding height profile along the given line; (c) SEM image for freeze-fractured cross-sections of graphene/PMMA composite at 2.08 vol % loading and the proposed dispersion pattern of graphene sheets in the matrix; and (d) Electrical conductivity (σ_c) versus filler volume fraction (ϕ) for the composites. Inset shows a log-log plot of σ_c versus $(\phi - \phi_c)/(1 - \phi_c)$. Reproduced with permission from [62]. Copyright 2012 the Royal Society of Chemistry.



3.4. Cellulose Composites

3.4.1. With Carbon Nanotubes

Cellulose is structurally a linear polymer of cellobiose. It is the most abundant natural polymer in nature and consequently, represents the most promising renewable resource for biocomposites [139]. However, cellulose is generally difficult to process in solution or as a melt because of its strong intra- and inter-molecular hydrogen bonding between the individual chains. Fortunately, some specific ILs are found to be powerful solvents for cellulose [140–142]. As described above, CNTs also show good dispersion and stabilization in Imi-ILs. Many research groups have successfully prepared the nanotube cellulose composites with the assistance of Imi-ILs. Lu *et al.* [143] reported the facile preparation of the SWCNT/cellulose composite. Initially, SWCNTs were mixed with an Imi-IL of 1-butyl-3-methylimidazolium bromide (BmimBr) by ultrasonication at 80 °C for 20 min. To this mixture was then added a stock solution of cellulose in BmimBr and sonicated for another 10 min to give a well-dispersed black suspension. The SWCNT/cellulose composite was finally isolated after removal of BmimBr by repeated filtration and washing with water. It was found that SWCNTs were well wrapped by cellulose. This composite shows good biocompatibility and has potentials for the intracellular drug delivery and biomaterial scaffolds. Similarly, 1-butyl-3-methylimidazolium acetate (BmimAc) was also chosen to dissolve cellulose and disperse SWCNTs in turn [144]. The resulting SWCNT/cellulose composite was homogenous, hydrophilic, conductive and biocompatible, and could be utilized for the immobilization of leukemia K562 cells on a gold electrode to form an impedance cell sensor, showing a low detection limit.

In the work reported by Zhang *et al.* [145], AmimCl was used to fabricate the regenerated cellulose fibers reinforced with MWCNTs by dry-jet wet-spinning on a lab-scale spinneret assembly. It was found that MWCNTs were homogeneously dispersed within the cellulose matrix and aligned along the electrospun-fiber axis (see Figure 3 in [145]). The composite fiber with 4 wt % of MWCNTs has an electrical conductivity of $0.83 \text{ S}\cdot\text{m}^{-1}$, and its tensile strength and storage modulus increases by 40% and 2.5-fold, compared to the pure regenerated-cellulose fiber, respectively. This method can be used to fabricate the potential precursors of the cellulose-based carbon fibers. Linhardt *et al.* [146] have fabricated the core-sheath MWCNT-cellulose fibers by coaxial electrospinning from a solution of 1-methyl-3-methylimidazolium acetate (MmimAc). The electrospun fibers were collected in a coagulation bath of ethanol and water, and exhibit a conductivity of up to $10.7 \text{ S}\cdot\text{m}^{-1}$ at 45 wt % loading. The core-sheath conductive fibers could have potentials for the electrical double-layer supercapacitors and bimorph actuators.

3.4.2. With Graphene

Recently, Lu *et al.* [147] have reported the preparation of free-standing graphene/cellulose papers with the help of BmimCl. In their work, the ultrasonically-mixed suspension of BmimCl and GO aqueous dispersion was rotary evaporated to fully remove water. To this GO/BmimCl suspension was added an ammonia solution and a solution of cellulose in BmimCl, and the resulting mixture was heated at 80 °C for 12 h. A black precipitate was collected by filtration after adding water and re-dispersed in an aqueous solution of NaOH and thiourea under sonication. The final product was purified by washing with the precooled NaOH/thiourea solution and water under high-speed centrifugation to remove

un-adsorbed cellulose and BmimCl. It was found that cellulose could effectively reduce GO in BmimCl and subsequently stacked onto the basal planes of RGO. The highly-ordered graphene/cellulose paper fabricated by vacuum filtration improved the cell biocompatibility of graphene, and might have potential applications in biomaterial scaffolds for tissue engineering and medical devices. An Imi-IL of 1-ethyl-3-methylimidazolium acetate (EmimAc) was used by Mahmoudian *et al.* [148] to prepare graphene/cellulose composite films using solution casting method. Well-dispersed graphene nanoplatelets were found to have strong interaction with the regenerated cellulose. With the addition of 3 wt % of graphene, the tensile strength and Young's modulus increase by 34% and 56% for the composite films, respectively. The composite films also improve the gas-barrier of O₂ and CO₂ as well as water absorption resistance compared to the cellulose film.

4. Poly(ionic liquid) Composites

Poly(ionic liquid)s or polymeric/polymerized ionic liquids (PILs), produced by polymerization of ionic liquid monomers, can be considered as a special type of polyelectrolytes containing IL repeating units in each polymer chain [149]. The major advantages of PILs over ILs are the improvements in the mechanical stability, processability, durability, and spatial controllability [150]. However, almost all PILs are solid in nature near room temperature, but generally have an observable T_g as opposed to conventional solid polyelectrolytes [151]. PILs combine the excellent properties of ILs with the macromolecular architectures and hence possess new functions and applications [152]. In the last decade, PILs have attracted great attention in the fabrication of multifunctional composites containing CNTs or graphene sheets [63].

4.1. With Carbon Nanotubes

Fukushima *et al.* [59] first fabricated SWCNT/PIL composites by *in situ* free radical polymerization of 1-(4-acryloyloxybutyl)-3-methylimidazolium hexafluorophosphate (AmimPF₆) gel with SWCNTs in the presence of 2,2'-azobisisobutyronitrile. The resulting composite film filled by 3.8 wt % of SWCNTs shows an electrical conductivity of 0.56 S·cm⁻¹ and a nearly 400% increase in dynamic hardness in comparison with pure PILs. They used the same method to prepare a series of plastic films by polymerization of Imi-ILs in the presence of SWCNTs [153]. Kim *et al.* [154] reported the preparation of SWCNT/PIL gels by *in situ* radical polymerization of 1-vinyl-3-ethylimidazolium bromide (VeimBr) in the presence of oxidized nanotubes. The use of polymerizable Imi-ILs as the gelling medium allows for the fabrication of well-dispersed SWCNT/polymer composites, which show drastic improvements in the mechanical, thermal and electrical properties. Chen *et al.* [155] found that PILs uniformly coated the surface of MWCNTs by radical polymerization of VeimBr. The resulting MWCNT/poly(VeimBr) gels show superior electrocatalytic activity for reduction of O₂ and H₂O₂ compared to pristine MWCNTs. Such soft materials have potential applications for the elastic conductors, flexible electrodes, antistatic coating materials, and sensors.

Mecerreyes *et al.* [156] directly used poly(VeimBr) to stably disperse SWCNTs in solvents. In the work reported by Dubios *et al.* [157], an imidazolium end-functionalized poly(L-lactide) (Imi-PLLA) was synthesized by ring-opening polymerization of L-lactide in the presence of a hydroxylated IL as an initiator, and then was used to assist dispersion of MWCNTs into chloroform. The homogeneous

suspension of MWCNTs exists over a period of about two months, due to the high binding ability of imidazolium moieties of Imi-PLLA with the conjugated surface of MWCNTs. In contrast, MWCNTs precipitate quickly from the chloroform solution of pyrene and anthracene end-functionalized PLLA. The use of imidazolium-based PILs provides an efficient and reliable strategy for the homogeneous dispersion of CNTs in solvents and subsequent in the polymer matrix.

Chen *et al.* [158] used the poly(VeimBF₄)-coated MWCNTs to serve as the supported templates for the uniform deposition of Pt or PtRu nanoparticles with an average diameter of ~1.9 nm for Pt and ~1.3 nm for PtRu. The resulting nanohybrids show highly electrocatalytic properties in the direct oxidation of methanol and hence, are a promising catalyst support in fuel cells. A polyethylenimine-functionalized Imi-IL was also applied to fabricate a novel biosensor based on the MWCNT-Au-PIL-glucose oxidase (GOD) thin film at a glass carbon electrode, which retains the good bioactivity of GOD and exhibits a high electrochemical response to glucose [159]. In fact, ILs have been actively utilized for the fabrication of metal nanoparticles because of their high coordination abilities toward metal ions [160]. CNTs have proved to be excellent nanoparticle supports due to high specific surface of 1D geometry [161]. These combined advantages of PILs and CNTs would allow developing the multifunctional nanohybrids for applications in catalysts, sensors, fuel cells and optoelectronics.

4.2. With Graphene

The PIL of poly(VbimCl) is first used to stably disperse RGO sheets in BmimPF₆ [61]. Similarly, poly(VeimBr)-modified graphene sheets were obtained by chemical reduction of GO with hydrazine monohydrate in the presence of poly(VeimBr) [162]. They are finely dispersed for 6 months without any agglomeration in an aqueous solution, and can be readily transferred into an organic phase (e.g., propylene carbonate, DMF and NMP) by ion-exchange with hydrophobic anions such as Tf₂N. This shows a tunable solubilizing characteristic of graphene in the aqueous and organic phases. Ruoff *et al.* [163] fabricated a high-performance supercapacitor assembled with an electrode of poly(1-vinyl-3-ethylimidazolium) bis(trifluoromethylsulfonyl)amide [poly(VeimTf₂N)] modified graphene films and a compatible electrolyte of EmimTf₂N. The supercapacitor has a stable electrochemical response, and shows high energy density, power density and specific capacitance (up to 6.5 Wh·kg⁻¹, 2.4 kW·kg⁻¹ and 187 F·g⁻¹, respectively).

The PIL of poly(1-vinyl-3-butylimidazolium bromide) poly(VbimBr) was used to functionalize graphene sheets, thus showing a strong positive charge [164]. The negatively charged GOD was then immobilized onto the functionalized graphene sheets to form a GOD/poly(VbimBr)-graphene/glassy carbon electrode, which greatly improves the electrocatalytic properties of glucose oxidation with good sensitivity and wide linear range. Recently, Wang *et al.* [165] fabricated a nonenzymatic sensor for H₂O₂ based on the electrodeposition of Ag nanoparticles onto the film of poly(VeimTf₂N)-stabilized graphene sheets. The as-fabricated sensor shows good linear response in the range of 0.1 μM to 2.2 mM of H₂O₂ and low detection limit (0.05 μM). Therefore, PIL-mediated graphene may provide a promising platform for the fabrication of biosensors and other electrochemical devices.

A graphene/polyaniline (PANI) composite was successfully prepared by *in situ* chemical oxidative polymerization of aniline with the aid of poly(VbimCl) which helps stabilizing graphene sheets in water [166]. The electrical conductivity of the composite with 21 wt % loading significantly increases to 75 S·m⁻¹ from 15 S·m⁻¹ of pure PANI. Similarly, graphene/poly(3,4-ethylenedioxythiophene) (PEDT)

composites were fabricated by chemical oxidative polymerization of 3,4-ethylenedioxythiophene in the presence of poly(VeimTf₂N)-modified graphene [167]. Poly(VeimTf₂N) was here found to be absorbed and subsequently promoted PEDT growth onto the surface of graphene sheets. The resulting composite shows an electrical conductivity of up to 18.8 S·cm⁻¹ at 0.3 wt % loading, and its thin film on glass substrate has a surface resistivity as low as 1.8 × 10⁴ Ω·sq⁻¹ at an optical transmittance of 91.18%. Lonkar *et al.* [168] found that hydroxyl-ended Imi-ILs could be attached to the surface of graphene, and then initiated *in situ* ring-opening polymerization of ε-caprolactone to produce graphene/PCL composites. Graphene sheets are well dispersed in the matrix and thus contribute to a significant increase in the storage modulus compared to PCL. These graphene/polymer composites have potential applications in energy storage, optoelectronics, electromagnetic shielding and antistatic coatings.

5. Conclusions

Imi-ILs have surface tensions closely matching the surface energy of graphitic layer and interact non-covalently with the conjugated graphitic surface through π-π and/or cation-π stacking. Therefore, Imi-ILs have been successfully used as dispersants and stabilizers for untangling CNTs and exfoliating graphene sheets in solvents. Imi-ILs also show a potential for microwave reduction of GO due to their low vapor pressure, high thermal stability and strong microwave absorption ability. Such advantages have made Imi-ILs promising applications in the fabrication of nanotube and graphene polymer composites over the past decade. Large evidences have been accumulated indicating that Imi-ILs not only facilitate homogeneous dispersion of CNTs and graphene in the polymer matrix, and enhance interface adhesion between two components, but also endow the final composites with new functions.

The as-prepared polymer conductive composites show great potential applications for fully plastic actuators, electrochemical devices, flexible supercapacitors, polymer electrolyte fuel cells and solar cells, as well as elastic conductors for large-area electronic integrated circuits on the arbitrary curved surfaces and movable parts. In particular, cellulose is natural, inexpensive, renewable, nontoxic and biodegradable, and also is capable of being soluble in some Imi-ILs. The presence of Imi-ILs accelerates simultaneously the dispersion of CNTs, graphene and dissolution of cellulose. The fabricated biocomposites combine the biocompatibility of cellulose and multi-functionality of CNTs and graphene, and would be used as scaffolds, biosensors, drug carriers and biological transporters.

However, there is still a question about the ability to produce large quantities of individual CNTs or monolayer graphene sheets through direct exfoliation of graphite in Imi-ILs. In addition, only some fluoropolymers, hydrocarbon polymers, and polyacrylates that have been succeeded in producing nanotube and graphene polymer composites with the aid of Imi-ILs. Future attempts should perhaps focus on the use of new Imi-ILs in conjunction with the improved methods, which help to exfoliate individually CNTs or graphene sheets into solvents or much more kinds of polymers.

Acknowledgments

The authors acknowledge financial support from the National Natural Science Foundation of China (51073050, 51273057 and 51210004), the Program for New Century Excellent Talents in University (NCET-12-0709), the Key Project of Science and Technology from Ministry of Education of China (210131), the Open Project of State Key Laboratory of Materials Processing and Die & Mould

Technology (2012-P10) at Huazhong University of Science and Technology, and Wuhan Science and Technology Bureau of China (201050231088).

Conflict of interest

The authors declare no conflict of interest.

References

1. Winey, K.I.; Vaia, R.A. Polymer nanocomposites. *MRS Bull.* **2007**, *32*, 314–322.
2. Baughman, R.H.; Zakhidov, A.A.; de Heer, W.A. Carbon nanotubes—The route toward applications. *Science* **2002**, *297*, 787–792.
3. Byrne, M.T.; Gun'ko, Y.K. Recent advances in research on carbon nanotube—Polymer composites. *Adv. Mater.* **2010**, *22*, 1672–1688.
4. Ajayan, P.M.; Tour, J.M. Materials science: Nanotube composites. *Nature* **2007**, *447*, 1066–1068.
5. Singh, V.; Joung, D.; Zhai, L.; Das, S.; Khondaker, S.I.; Seal, S. Graphene based materials: Past, present and future. *Prog. Mater. Sci.* **2011**, *56*, 1178–1271.
6. Verdejo, R.; Bernal, M.M.; Romasanta, L.J.; Lopez-Manchado, M.A. Graphene filled polymer nanocomposites. *J. Mater. Chem.* **2011**, *21*, 3301–3310.
7. Novoselov, K.S. Electric field effect in atomically thin carbon films. *Science* **2004**, *306*, 666–669.
8. Allen, M.J.; Tung, V.C.; Kaner, R.B. Honeycomb carbon: A review of graphene. *Chem. Rev.* **2010**, *110*, 132–145.
9. Iijima, S. Helical microtubules of graphitic carbon. *Nature* **1991**, *354*, 56–58.
10. Iijima, S.; Ichihashi, T. Single-shell carbon nanotubes of 1-nm diameter. *Nature* **1993**, *363*, 603–605.
11. Bethune, D.S.; Kiang, C.H.; Devries, M.S.; Gorman, G.; Savoy, R.; Vazquez, J.; Beyers, R. Cobalt-catalyzed growth of carbon nanotubes with single-atomic-layerwalls. *Nature* **1993**, *363*, 605–607.
12. Yu, M.F.; Lourie, O.; Dyer, M.J.; Moloni, K.; Kelly, T.F.; Ruoff, R.S. Strength and breaking mechanism of multiwalled carbon nanotubes under tensile load. *Science* **2000**, *287*, 637–640.
13. Berber, S.; Kwon, Y.K.; Tomanek, D. Unusually high thermal conductivity of carbon nanotubes. *Phys. Rev. Lett.* **2000**, *84*, 4613–4616.
14. Durkop, T.; Getty, S.A.; Cobas, E.; Fuhrer, M.S. Extraordinary mobility in semiconducting carbon nanotubes. *Nano Lett.* **2004**, *4*, 35–39.
15. Lee, C.; Wei, X.D.; Kysar, J.W.; Hone, J. Measurement of the elastic properties and intrinsic strength of monolayer graphene. *Science* **2008**, *321*, 385–388.
16. Du, X.; Skachko, I.; Barker, A.; Andrei, E.Y. Approaching ballistic transport in suspended graphene. *Nat. Nanotechnol.* **2008**, *3*, 491–495.
17. Balandin, A.A.; Ghosh, S.; Bao, W.; Calizo, I.; Teweldebrhan, D.; Miao, F.; Lau, C.N. Superior thermal conductivity of single-layer graphene. *Nano Lett.* **2008**, *8*, 902–907.
18. Stoller, M.D.; Park, S.J.; Zhu, Y.W.; An, J.H.; Ruoff, R.S. Graphene-based ultracapacitors. *Nano Lett.* **2008**, *8*, 3498–3502.
19. Nair, R.R.; Blake, P.; Grigorenko, A.N.; Novoselov, K.S.; Booth, T.J.; Stauber, T.; Peres, N.M.R.; Geim, A.K. Fine structure constant defines visual transparency of graphene. *Science* **2008**, *320*, 1308–1308.

20. Bae, S.; Kim, H.; Lee, Y.; Xu, X.F.; Park, J.S.; Zheng, Y.; Balakrishnan, J.; Lei, T.; Kim, H.R.; Song, Y.I.; *et al.* Roll-to-roll production of 30-inch graphene films for transparent electrodes. *Nat. Nanotechnol.* **2010**, *5*, 574–578.
21. Kuilla, T.; Bhadra, S.; Yao, D.; Kim, N.H.; Bose, S.; Lee, J.H. Recent advances in graphene based polymer composites. *Prog. Polym. Sci.* **2010**, *35*, 1350–1375.
22. Kim, H.; Abdala, A.A.; Macosko, C.W. Graphene/polymer nanocomposites. *Macromolecules* **2010**, *43*, 6515–6530.
23. Xie, X.L.; Mai, Y.-W.; Zhou, X.P. Dispersion and alignment of carbon nanotubes in polymer matrix: A review. *Mater. Sci. Eng. R Rep.* **2005**, *49*, 89–112.
24. Cheng, Q.; Bao, J.; Park, J.; Liang, Z.; Zhang, C.; Wang, B. High mechanical performance composite conductor: Multi-walled carbon nanotube sheet/bismaleimide nanocomposites. *Adv. Funct. Mater.* **2009**, *19*, 3219–3225.
25. Yuan, W.; Che, J.F.; Chan-Park, M.B. A novel polyimide dispersing matrix for highly electrically conductive solution-cast carbon nanotube-based composite. *Chem. Mater.* **2011**, *23*, 4149–4157.
26. Lin, H.; Li, L.; Ren, J.; Cai, Z.; Qiu, L.; Yang, Z.; Peng, H. Conducting polymer composite film incorporated with aligned carbon nanotubes for transparent, flexible and efficient supercapacitor. *Sci. Rep.* **2013**, *3*, doi:10.1038/srep01353.
27. Kim, S.N.; Rusling, J.F.; Papadimitrakopoulos, F. Carbon nanotubes for electronic and electrochemical detection of biomolecules. *Adv. Mater.* **2007**, *19*, 3214–3228.
28. Lu, F.; Gu, L.; Meziani, M.J.; Wang, X.; Luo, P.G.; Veca, L.M.; Cao, L.; Sun, Y.-P. Advances in bioapplications of carbon nanotubes. *Adv. Mater.* **2009**, *21*, 139–152.
29. Lu, L.; Chen, W. Biocompatible composite actuator: A supramolecular structure consisting of the biopolymer chitosan, carbon nanotubes, and an ionic Liquid. *Adv. Mater.* **2010**, *22*, 3745–3748.
30. Koerner, H.; Price, G.; Pearce, N.A.; Alexander, M.; Vaia, R.A. Remotely actuated polymer nanocomposites—Stress-recovery of carbon-nanotube-filled thermoplastic elastomers. *Nat. Mater.* **2004**, *3*, 115–120.
31. Ahir, S.V.; Terentjev, E.M. Photomechanical actuation in polymer-nanotube composites. *Nat. Mater.* **2005**, *4*, 491–495.
32. Hasan, T.; Sun, Z.; Wang, F.; Bonaccorso, F.; Tan, P.H.; Rozhin, A.G.; Ferrari, A.C. Nanotube-polymer composites for ultrafast photonics. *Adv. Mater.* **2009**, *21*, 3874–3899.
33. Park, H.; Brown, P.R.; Bulović, V.; Kong, J. Graphene as transparent conducting electrodes in organic photovoltaics: Studies in graphene morphology, hole transporting layers, and counter electrodes. *Nano Lett.* **2011**, *12*, 133–140.
34. Ren, S.Q.; Bernardi, M.; Lunt, R.R.; Bulovic, V.; Grossman, J.C.; Gradecak, S. Toward efficient carbon nanotube/P3HT solar cells: Active layer morphology, electrical, and optical properties. *Nano Lett.* **2011**, *11*, 5316–5321.
35. Han, J.; Kim, H.; Kim, D.Y.; Jo, S.M.; Jang, S.Y. Water-soluble polyelectrolyte-grafted multiwalled carbon nanotube thin films for efficient counter electrode of dye-sensitized solar cells. *ACS Nano* **2010**, *4*, 3503–3509.
36. Hellstrom, S.L.; Lee, H.W.; Bao, Z.N. Polymer-assisted direct deposition of uniform carbon nanotube bundle networks for high performance transparent electrodes. *ACS Nano* **2009**, *3*, 1423–1430.

37. Huang, S.Q.; Li, L.; Yang, Z.B.; Zhang, L.L.; Saiyin, H.; Chen, T.; Peng, H.S. A new and general fabrication of an aligned carbon nanotube/polymer film for electrode applications. *Adv. Mater.* **2011**, *23*, 4707–4710.
38. Yang, Y.K.; Xie, X.L.; Mai, Y.-W. Functionalization of Carbon Nanotubes for Polymer Nanocomposites. In *Functionalization of Carbon Nanotubes for Polymer Nanocomposites: Synthesis, Properties and Applications*; McNally, T., Pötschke, P., Eds.; Woodhead Publishing Ltd.: Cambridge, UK, 2011; pp. 55–91.
39. Yang, Y.K.; Xie, X.L.; Cui, W. Functionalization of Carbon Nanotubes with Ionic Liquids. In *Green Solvents II: Properties and Applications in Chemistry*; Mohammad, A., Inamuddin, Ed.; Springer Dordrecht Heidelberg: New York, London, 2012; pp. 399–434.
40. Yang, Y.K.; Qiu, S.Q.; Wang, X.B.; Xie, X.L. Functionalization and structure control of carbon nanotubes with polymers: Polymer-grafted carbon nanotubes. *Prog. Chem.* **2010**, *22*, 684–695.
41. Kaiser, A.B.; Skakalova, V. Electronic conduction in polymers, carbon nanotubes and graphene. *Chem. Soc. Rev.* **2011**, *40*, 3786–3801.
42. Yang, Y.K.; Qiu, S.Q.; Xie, X.L.; Wang, X.B.; Li, R.K.Y. A facile, green, and tunable method to functionalize carbon nanotubes with water-soluble azo initiators by one-step free radical addition. *Appl. Surf. Sci.* **2010**, *256*, 3286–3292.
43. Yang, Y.K.; Yu, L.J.; Peng, R.G.; Huang, Y.L.; He, C.E.; Liu, H.Y.; Wang, X.B.; Xie, X.L.; Mai, Y.-W. Incorporation of liquid-like multiwalled carbon nanotubes into an epoxy matrix by solvent-free processing. *Nanotechnology* **2012**, *23*, e225701.
44. Yang, Y.K.; Xie, X.L.; Wu, J.G.; Mai, Y.W. Synthesis and self-assembly of polystyrene-grafted multiwalled carbon nanotubes with a hairy-rod nanostructure. *J. Polym. Sci. Polym. Chem.* **2006**, *44*, 3869–3881.
45. Yang, Y.K.; Mao, L.B.; Xie, X.L.; Mai, Y.W. Liquid crystallinity and novel assembly of amorphous polymer grafted carbon nanotubes. *Solid State Phenom.* **2007**, 1411–1414.
46. Yang, Y.K.; Xie, X.L.; Wu, J.G.; Yang, Z.F.; Wang, X.T.; Mai, Y.W. Multiwalled carbon nanotubes functionalized by hyperbranched poly(urea-urethane)s by a one-pot polycondensation. *Macromol. Rapid Comm.* **2006**, *27*, 1695–1701.
47. Yang, Y.K.; Xie, X.L.; Yang, Z.F.; Wang, X.T.; Cui, W.; Yang, J.Y.; Mai, Y.W. Controlled synthesis and novel solution rheology of hyperbranched poly(urea-urethane)-functionalized multiwalled carbon nanotubes. *Macromolecules* **2007**, *40*, 5858–5867.
48. Yang, Y.K.; Tsui, C.P.; Tang, C.Y.; Qiu, S.Q.; Zhao, Q.; Cheng, X.J.; Sun, Z.G.; Li, R.K.Y.; Xie, X.L. Functionalization of carbon nanotubes with biodegradable supramolecular polypseudorotaxanes from grafted-poly(ϵ -caprolactone) and α -cyclodextrins. *Eur. Polym. J.* **2010**, *46*, 145–155.
49. Yang, Y.K.; Qiu, S.Q.; He, C.G.; He, W.J.; Yu, L.J.; Xie, X.L. Green chemical functionalization of multiwalled carbon nanotubes with poly(ϵ -caprolactone) in ionic liquids. *Appl. Surf. Sci.* **2010**, *257*, 1010–1014.
50. Yang, Y.K.; Wang, X.T.; Liu, L.; Xie, X.L.; Yang, Z.F.; Li, R.K.Y.; Mai, Y.W. Structure and photoresponsive behaviors of multiwalled carbon nanotubes grafted by polyurethanes containing azobenzene side chains. *J. Phys. Chem. C* **2007**, *111*, 11231–11239.

51. Du, F.P.; Wu, K.B.; Yang, Y.K.; Liu, L.; Gan, T.; Xie, X.L. Synthesis and electrochemical probing of water-soluble poly(sodium 4-styrenesulfonate-co-acrylic acid)-grafted multiwalled carbon nanotubes. *Nanotechnology* **2008**, *19*, e085716.
52. Zhang, R.H.; Yang, Y.K.; Xie, X.L.; Li, R.K.Y. Dispersion and crystallization studies of hyper-branched poly(urea-urethane)s-grafted carbon nanotubes filled polyamide-6 nanocomposites. *Compos. A* **2010**, *41*, 670–677.
53. Cui, W.; Du, F.P.; Zhao, J.C.; Zhang, W.; Yang, Y.K.; Xie, X.L.; Mai, Y.-W. Improving thermal conductivity while retaining high electrical resistivity of epoxy composites by incorporating silica-coated multi-walled carbon nanotubes. *Carbon* **2011**, *49*, 495–500.
54. Weingärtner, H. Understanding ionic liquids at the molecular level: Facts, problems, and controversies. *Angew. Chem. Int. Ed.* **2008**, *47*, 654–670.
55. Greaves, T.L.; Drummond, C.J. Protic ionic liquids: Properties and applications. *Chem. Rev.* **2007**, *108*, 206–237.
56. Lu, J.; Yan, F.; Texter, J. Advanced applications of ionic liquids in polymer science. *Prog. Polym. Sci.* **2009**, *34*, 431–448.
57. Greaves, T.L.; Drummond, C.J. Ionic liquids as amphiphile self-assembly media. *Chem. Soc. Rev.* **2008**, *37*, 1709–1726.
58. Antonietti, M.; Kuang, D.; Smarsly, B.; Zhou, Y. Ionic liquids for the convenient synthesis of functional nanoparticles and other inorganic nanostructures. *Angew. Chem. Int. Ed.* **2004**, *43*, 4988–4992.
59. Fukushima, T.; Kosaka, A.; Ishimura, Y.; Yamamoto, T.; Takigawa, T.; Ishii, N.; Aida, T. Molecular ordering of organic molten salts triggered by single-walled carbon nanotubes. *Science* **2003**, *300*, 2072–2074.
60. Price, B.K.; Hudson, J.L.; Tour, J.M. Green chemical functionalization of single-walled carbon nanotubes in ionic liquids. *J. Am. Chem. Soc.* **2005**, *127*, 14867–14870.
61. Zhou, X.S.; Wu, T.B.; Ding, K.L.; Hu, B.J.; Hou, M.Q.; Han, B.X. Dispersion of graphene sheets in ionic liquid bmim PF6 stabilized by an ionic liquid polymer. *Chem. Commun.* **2010**, *46*, 386–388.
62. Yang, Y.K.; He, C.E.; Peng, R.G.; Baji, A.; Du, X.S.; Huang, Y.L.; Xie, X.L.; Mai, Y.-W. Non-covalently modified graphene sheets by imidazolium ionic liquids for multifunctional polymer nanocomposites. *J. Mater. Chem.* **2012**, *22*, 5666–5675.
63. Fukushima, T.; Aida, T. Ionic liquids for soft functional materials with carbon nanotubes. *Chem. Eur. J.* **2007**, *13*, 5048–5058.
64. Ausman, K.D.; Piner, R.; Lourie, O.; Ruoff, R.S.; Korobov, M. Organic solvent dispersions of single-walled carbon nanotubes: Toward solutions of pristine nanotubes. *J. Phys. Chem. B* **2000**, *104*, 8911–8915.
65. Furtado, C.A.; Kim, U.J.; Gutierrez, H.R.; Pan, L.; Dickey, E.C.; Eklund, P.C. Debundling and dissolution of single-walled carbon nanotubes in amide solvents. *J. Am. Chem. Soc.* **2004**, *126*, 6095–6105.
66. Bahr, J.L.; Mickelson, E.T.; Bronikowski, M.J.; Smalley, R.E.; Tour, J.M. Dissolution of small diameter single-wall carbon nanotubes in organic solvents? *Chem. Commun.* **2001**, *2*, 193–194.
67. Giordani, S.; Bergin, S.D.; Nicolosi, V.; Lebedkin, S.; Kappes, M.M.; Blau, W.J.; Coleman, J.N. Debundling of single-walled nanotubes by dilution: Observation of large populations of individual nanotubes in amide solvent dispersions. *J. Phys. Chem. B* **2006**, *110*, 15708–15718.

68. Landi, B.J.; Ruf, H.J.; Worman, J.J.; Raffaele, R.P. Effects of alkyl amide solvents on the dispersion of single-wall carbon nanotubes. *J. Phys. Chem. B* **2004**, *108*, 17089–17095.
69. Cheng, Q.; Debnath, S.; Gregan, E.; Byrne, H.J. Effect of solvent solubility parameters on the dispersion of single-walled carbon nanotubes. *J. Phys. Chem. C* **2008**, *112*, 20154–20158.
70. Kim, D.S.; Nepal, D.; Geckeler, K.E. Individualization of single-walled carbon nanotubes: Is the solvent important? *Small* **2005**, *1*, 1117–1124.
71. Cheng, Q.; Debnath, S.; O'Neill, L.; Hedderman, T.G.; Gregan, E.; Byrne, H.J. Systematic study of the dispersion of SWNTs in organic solvents. *J. Phys. Chem. C* **2010**, *114*, 4857–4863.
72. Coleman, J.N. Liquid-phase exfoliation of nanotubes and graphene. *Adv. Funct. Mater.* **2009**, *19*, 3680–3695.
73. Hallett, J.P.; Welton, T. Room-temperature ionic liquids: Solvents for synthesis and catalysis. *Chem. Rev.* **2011**, *111*, 3508–3576.
74. Bellayer, S.; Gilman, J.W.; Eidelman, N.; Bourbigot, S.; Flambard, X.; Fox, D.M.; de Long, H.C.; Trulove, P.C. Preparation of homogeneously dispersed multiwalled carbon nanotube/polystyrene nanocomposites via melt extrusion using trialkyl imidazolium compatibilizer. *Adv. Funct. Mater.* **2005**, *15*, 910–916.
75. Shim, Y.; Kim, H.J. Solvation of carbon nanotubes in a room-temperature ionic liquid. *ACS Nano* **2009**, *3*, 1693–1702.
76. Wang, J.Y.; Chu, H.B.; Li, Y. Why single-walled carbon nanotubes can be dispersed in imidazolium-based ionic liquids. *ACS Nano* **2008**, *2*, 2540–2546.
77. Di Crescenzo, A.; Demurtas, D.; Renzetti, A.; Siani, G.; de Maria, P.; Meneghetti, M.; Prato, M.; Fontana, A. Disaggregation of single-walled carbon nanotubes (SWNTs) promoted by the ionic liquid-based surfactant 1-hexadecyl-3-vinyl-imidazolium bromide in aqueous solution. *Soft Matter* **2009**, *5*, 62–66.
78. Zhang, Y.J.; Shen, Y.F.; Li, J.H.; Niu, L.; Dong, S.J.; Ivaska, A. Electrochemical functionalization of single-walled carbon nanotubes in large quantities at a room-temperature ionic liquid supported three-dimensional network electrode. *Langmuir* **2005**, *21*, 4797–4800.
79. Ahmad, S.; Singh, S. Electrochromic device based on carbon nanotubes functionalized poly (methyl pyrrole) synthesized in hydrophobic ionic liquid medium. *Electrochem. Commun.* **2008**, *10*, 895–898.
80. Wei, D.; Kvarnstrom, C.; Lindfors, T.; Ivaska, A. Electrochemical functionalization of single walled carbon nanotubes with polyaniline in ionic liquids. *Electrochem. Commun.* **2007**, *9*, 206–210.
81. Cai, M.; Thorpe, D.; Adamson, D.H.; Schniepp, H.C. Methods of graphite exfoliation. *J. Mater. Chem.* **2012**, *22*, 24992–25002.
82. Park, S.; Ruoff, R.S. Chemical methods for the production of graphenes. *Nat. Nanotechnol.* **2009**, *4*, 217–224.
83. Pei, S.; Cheng, H.M. The reduction of graphene oxide. *Carbon* **2012**, *50*, 3210–3228.
84. Wang, H.; Robinson, J.T.; Li, X.; Dai, H. Solvothermal reduction of chemically exfoliated graphene sheets. *J. Am. Chem. Soc.* **2009**, *131*, 9910–9911.
85. Compton, O.C.; Jain, B.; Dikin, D.A.; Abouimrane, A.; Amine, K.; Nguyen, S.T. Chemically active reduced graphene oxide with tunable C/O ratios. *ACS Nano* **2011**, *5*, 4380–4391.

86. Liang, Y.T.; Vijayan, B.K.; Gray, K.A.; Hersam, M.C. Minimizing graphene defects enhances titania nanocomposite-based photocatalytic reduction of Co(II) for improved solar fuel production. *Nano Lett.* **2011**, *11*, 2865–2870.
87. Viet, H.P.; Tran, V.C.; Hur, S.H.; Oh, E.; Kim, E.J.; Shin, E.W.; Chung, J.S. Chemical functionalization of graphene sheets by solvothermal reduction of a graphene oxide suspension in *N*-methyl-2-pyrrolidone. *J. Mater. Chem.* **2011**, *21*, 3371–3377.
88. Dubin, S.; Gilje, S.; Wang, K.; Tung, V.C.; Cha, K.; Hall, A.S.; Farrar, J.; Varshneya, R.; Yang, Y.; Kaner, R.B. A one-step, solvothermal reduction method for producing reduced graphene oxide dispersions in organic solvents. *ACS Nano* **2010**, *4*, 3845–3852.
89. Chen, W.F.; Yan, L.F.; Bangal, P.R. Preparation of graphene by the rapid and mild thermal reduction of graphene oxide induced by microwaves. *Carbon* **2010**, *48*, 1146–1152.
90. Zhu, Y.; Stoller, M.D.; Cai, W.; Velamakanni, A.; Piner, R.D.; Chen, D.; Ruoff, R.S. Exfoliation of graphite oxide in propylene carbonate and thermal reduction of the resulting graphene oxide platelets. *ACS Nano* **2010**, *4*, 1227–1233.
91. Keeley, G.P.; O'Neill, A.; McEvoy, N.; Peltekis, N.; Coleman, J.N.; Duesberg, G.S. Electrochemical ascorbic acid sensor based on DMF-exfoliated graphene. *J. Mater. Chem.* **2010**, *20*, 7864–7869.
92. Zhao, W.F.; Fang, M.; Wu, F.R.; Wu, H.; Wang, L.W.; Chen, G.H. Preparation of graphene by exfoliation of graphite using wet ball milling. *J. Mater. Chem.* **2010**, *20*, 5817–5819.
93. Choi, E.K.; Jeon, I.Y.; Bae, S.Y.; Lee, H.J.; Shin, H.S.; Dai, L.M.; Baek, J.B. High-yield exfoliation of three-dimensional graphite into two-dimensional graphene-like sheets. *Chem. Commun.* **2010**, *46*, 6320–6322.
94. Hernandez, Y.; Nicolosi, V.; Lotya, M.; Blighe, F.M.; Sun, Z.Y.; De, S.; McGovern, I.T.; Holland, B.; Byrne, M.; Gun'ko, Y.K.; *et al.* High-yield production of graphene by liquid-phase exfoliation of graphite. *Nat. Nanotechnol.* **2008**, *3*, 563–568.
95. Hamilton, C.E.; Lomeda, J.R.; Sun, Z.Z.; Tour, J.M.; Barron, A.R. High-yield organic dispersions of unfunctionalized graphene. *Nano Lett.* **2009**, *9*, 3460–3462.
96. Lotya, M.; Hernandez, Y.; King, P.J.; Smith, R.J.; Nicolosi, V.; Karlsson, L.S.; Blighe, F.M.; De, S.; Wang, Z.; McGovern, I.T.; *et al.* Liquid phase production of graphene by exfoliation of graphite in surfactant/water solutions. *J. Am. Chem. Soc.* **2009**, *131*, 3611–3620.
97. Rangappa, D.; Sone, K.; Wang, M.; Gautam, U.K.; Golberg, D.; Itoh, H.; Ichihara, M.; Honma, I. Rapid and direct conversion of graphite crystals into high-yielding, good-quality graphene by supercritical fluid exfoliation. *Chem. Eur. J.* **2010**, *16*, 6488–6494.
98. Cui, X.; Zhang, C.Z.; Hao, R.; Hou, Y.L. Liquid-phase exfoliation, functionalization and applications of graphene. *Nanoscale* **2011**, *3*, 2118–2126.
99. Liu, N.; Luo, F.; Wu, H.X.; Liu, Y.H.; Zhang, C.; Chen, J. One-step ionic-liquid-assisted electrochemical synthesis of ionic-liquid-functionalized graphene sheets directly from graphite. *Adv. Funct. Mater.* **2008**, *18*, 1518–1525.
100. Lu, J.; Yang, J.X.; Wang, J.Z.; Lim, A.L.; Wang, S.; Loh, K.P. One-pot synthesis of fluorescent carbon nanoribbons, nanoparticles, and graphene by the exfoliation of graphite in ionic liquids. *ACS Nano* **2009**, *3*, 2367–2375.

101. Wang, X.Q.; Fulvio, P.F.; Baker, G.A.; Veith, G.M.; Unocic, R.R.; Mahurin, S.M.; Chi, M.F.; Dai, S. Direct exfoliation of natural graphite into micrometre size few layers graphene sheets using ionic liquids. *Chem. Commun.* **2010**, *46*, 4487–4489.
102. Nuvoli, D.; Valentini, L.; Alzari, V.; Scognamillo, S.; Bon, S.B.; Piccinini, M.; Illescas, J.; Mariani, A. High concentration few-layer graphene sheets obtained by liquid phase exfoliation of graphite in ionic liquid. *J. Mater. Chem.* **2011**, *21*, 3428–3431.
103. Shang, N.G.; Papakonstantinou, P.; Sharma, S.; Lubarsky, G.; Li, M.; McNeill, D.W.; Quinn, A.J.; Zhou, W.; Blackley, R. Controllable selective exfoliation of high-quality graphene nanosheets and nanodots by ionic liquid assisted grinding. *Chem. Commun.* **2012**, *48*, 1877–1879.
104. Safavi, A.; Tohidi, M.; Mahyari, F.A.; Shahbaazi, H. One-pot synthesis of large scale graphene nanosheets from graphite-liquid crystal composite via thermal treatment. *J. Mater. Chem.* **2012**, *22*, 3825–3831.
105. Lee, J.S.; Lee, T.; Song, H.K.; Cho, J.; Kim, B.S. Ionic liquid modified graphene nanosheets anchoring manganese oxide nanoparticles as efficient electrocatalysts for Zn-air batteries. *Energy Environ. Sci.* **2011**, *4*, 4148–4154.
106. Zhang, B.Q.; Ning, W.; Zhang, J.M.; Qiao, X.; Zhang, J.; He, J.S.; Liu, C.Y. Stable dispersions of reduced graphene oxide in ionic liquids. *J. Mater. Chem.* **2010**, *20*, 5401–5403.
107. Ji, Q.M.; Honma, I.; Paek, S.M.; Akada, M.; Hill, J.P.; Vinu, A.; Ariga, K. Layer-by-layer films of graphene and ionic liquids for highly selective gas sensing. *Angew. Chem. Int. Ed.* **2010**, *49*, 9737–9739.
108. Guo, C.X.; Lu, Z.S.; Lei, Y.; Li, C.M. Ionic liquid-graphene composite for ultratrace explosive trinitrotoluene detection. *Electrochem. Commun.* **2010**, *12*, 1237–1240.
109. Guo, S.J.; Wen, D.; Zhai, Y.M.; Dong, S.J.; Wang, E.K. Ionic liquid-graphene hybrid nanosheets as an enhanced material for electrochemical determination of trinitrotoluene. *Biosens. Bioelectron.* **2011**, *26*, 3475–3481.
110. Ng, S.R.; Guo, C.X.; Li, C.M. Highly sensitive nitric oxide sensing using three-dimensional graphene/ionic liquid nanocomposite. *Electroanalysis* **2011**, *23*, 442–448.
111. Shi, J.J.; Zhu, J.J. Sonochemical fabrication of Pd-graphene nanocomposite and its application in the determination of chlorophenols. *Electrochim. Acta* **2011**, *56*, 6008–6013.
112. Yang, M.H.; Choi, B.G.; Park, H.; Park, T.J.; Hong, W.H.; Lee, S.Y. Directed self-assembly of gold nanoparticles on graphene-ionic liquid hybrid for enhancing electrocatalytic activity. *Electroanalysis* **2011**, *23*, 850–857.
113. Peng, J.Y.; Hou, C.T.; Liu, X.X.; Li, H.B.; Hu, X.Y. Electrochemical behavior of azithromycin at graphene and ionic liquid composite film modified electrode. *Talanta* **2011**, *86*, 227–232.
114. Liu, Z.M.; Wang, Z.L.; Cao, Y.Y.; Jing, Y.F.; Liu, Y.L. High sensitive simultaneous determination of hydroquinone and catechol based on graphene/BMIMPF₆ nanocomposite modified electrode. *Sens. Actuators B* **2011**, *157*, 540–546.
115. Kim, T.; Kang, H.C.; Tung, T.T.; Lee, J.D.; Kim, H.; Yang, W.S.; Yoon, H.G.; Suh, K.S. Ionic liquid-assisted microwave reduction of graphite oxide for supercapacitors. *RSC Adv.* **2012**, *2*, 8808–8812.

116. Marquardt, D.; Vollmer, C.; Thomann, R.; Steurer, P.; Mulhaupt, R.; Redel, E.; Janiak, C. The use of microwave irradiation for the easy synthesis of graphene-supported transition metal nanoparticles in ionic liquids. *Carbon* **2011**, *49*, 1326–1332.
117. Shen, J.F.; Shi, M.; Yan, B.; Ma, H.W.; Li, N.; Ye, M.X. Ionic liquid-assisted one-step hydrothermal synthesis of TiO₂-reduced graphene oxide composites. *Nano Res.* **2011**, *4*, 795–806.
118. Shen, J.F.; Shi, M.; Yan, B.; Ma, H.W.; Li, N.; Ye, M.X. One-pot hydrothermal synthesis of Ag-reduced graphene oxide composite with ionic liquid. *J. Mater. Chem.* **2011**, *21*, 7795–7801.
119. Wang, S.; Zhang, Y.; Ma, H.L.; Zhang, Q.; Xu, W.; Peng, J.; Li, J.; Yu, Z.Z.; Zhai, M. Ionic-liquid-assisted facile synthesis of silver nanoparticle-reduced graphene oxide hybrids by gamma irradiation. *Carbon* **2013**, *55*, 245–252.
120. Fu, C.P.; Kuang, Y.F.; Huang, Z.Y.; Wang, X.; Du, N.N.; Chen, J.H.; Zhou, H.H. Electrochemical co-reduction synthesis of graphene/Au nanocomposites in ionic liquid and their electrochemical activity. *Chem. Phys. Lett.* **2010**, *499*, 250–253.
121. Yang, H.F.; Shan, C.S.; Li, F.H.; Han, D.X.; Zhang, Q.X.; Niu, L. Covalent functionalization of polydisperse chemically-converted graphene sheets with amine-terminated ionic liquid. *Chem. Commun.* **2009**, *26*, 3880–3882.
122. Shan, C.S.; Yang, H.F.; Han, D.X.; Zhang, Q.X.; Ivaska, A.; Niu, L. Electrochemical determination of NADH and ethanol based on ionic liquid-functionalized graphene. *Biosens. Bioelectron.* **2010**, *25*, 1504–1508.
123. Zhu, C.Z.; Guo, S.J.; Zhai, Y.M.; Dong, S.J. Layer-by-layer self-assembly for constructing a graphene/platinum nanoparticle three-dimensional hybrid nanostructure using ionic liquid as a linker. *Langmuir* **2010**, *26*, 7614–7618.
124. Landi, B.J.; Raffaele, R.P.; Heben, M.J.; Alleman, J.L.; van de Rveer, W.; Gennett, T. Single wall carbon nanotube-Nafion composite actuators. *Nano Lett.* **2002**, *2*, 1329–1332.
125. Fukushima, T.; Asaka, K.; Kosaka, A.; Aida, T. Fully plastic actuator through layer-by-layer casting with ionic-liquid-based bucky gel. *Angew. Chem. Int. Ed.* **2005**, *44*, 2410–2413.
126. Mukai, K.; Asaka, K.; Kiyohara, K.; Sugino, T.; Takeuchi, I.; Fukushima, T.; Aida, T. High performance fully plastic actuator based on ionic-liquid-based bucky gel. *Electrochim. Acta* **2008**, *53*, 5555–5562.
127. Takeuchi, I.; Asaka, K.; Kiyohara, K.; Sugino, T.; Terasawa, N.; Mukai, K.; Fukushima, T.; Aida, T. Electromechanical behavior of fully plastic actuators based on bucky gel containing various internal ionic liquids. *Electrochim. Acta* **2009**, *54*, 1762–1768.
128. Sugino, T.; Kiyohara, K.; Takeuchi, I.; Mukai, K.; Asaka, K. Actuator properties of the complexes composed by carbon nanotube and ionic liquid: The effects of additives. *Sens. Actuators B* **2009**, *141*, 179–186.
129. Takeuchi, I.; Asaka, K.; Kiyohara, K.; Sugino, T.; Terasawa, N.; Mukai, K.; Shiraishi, S. Electromechanical behavior of a fully plastic actuator based on dispersed nano-carbon/ionic-liquid-gel electrodes. *Carbon* **2009**, *47*, 1373–1380.
130. Sekitani, T.; Noguchi, Y.; Hata, K.; Fukushima, T.; Aida, T.; Someya, T. A rubberlike stretchable active matrix using elastic conductors. *Science* **2008**, *321*, 1468–1472.

131. Sekitani, T.; Nakajima, H.; Maeda, H.; Fukushima, T.; Aida, T.; Hata, K.; Someya, T. Stretchable active-matrix organic light-emitting diode display using printable elastic conductors. *Nat. Mater.* **2009**, *8*, 494–499.
132. Rogers, J.A.; Someya, T.; Huang, Y.G. Materials and mechanics for stretchable electronics. *Science* **2010**, *327*, 1603–1607.
133. Mandal, A.; Nandi, A.K. Ionic liquid integrated multiwalled carbon nanotube in a poly(vinylidene fluoride) matrix: Formation of a piezoelectric β -polymorph with significant reinforcement and conductivity improvement. *ACS Appl. Mater. Interfaces* **2013**, *5*, 747–760.
134. Pandey, G.P.; Rastogi, A.C. Graphene-based all-solid-state supercapacitor with ionic liquid gel polymer electrolyte. *MRS Proc.* **2012**, *1440*, doi:10.1557/opl.2012.1279.
135. Mitchell, C.A.; Bahr, J.L.; Arepalli, S.; Tour, J.M.; Krishnamoorti, R. Dispersion of functionalized carbon nanotubes in polystyrene. *Macromolecules* **2002**, *35*, 8825–8830.
136. Wei, D.; Baral, J.K.; Osterbacka, R.; Ivaska, A. Memory effect in an ionic liquid matrix containing single-walled carbon nanotubes and polystyrene. *Nanotechnology* **2008**, *19*, e055203.
137. Carrion, F.J.; Espejo, C.; Sanes, J.; Bermúdez, M.D. Single-walled carbon nanotubes modified by ionic liquid as antiwear additives of thermoplastics. *Compos. Sci. Technol.* **2010**, *70*, 2160–2167.
138. Zhao, L.; Li, Y.; Cao, X.; You, J.; Dong, W. Multifunctional role of an ionic liquid in melt-blended poly(methyl methacrylate)/multi-walled carbon nanotube nanocomposites. *Nanotechnology* **2012**, *23*, e255702.
139. Moon, R.J.; Martini, A.; Nairn, J.; Simonsen, J.; Youngblood, J. Cellulose nanomaterials review: Structure, properties and nanocomposites. *Chem. Soc. Rev.* **2011**, *40*, 3941–3994.
140. Pinkert, A.; Marsh, K.N.; Pang, S.S.; Staiger, M.P. Ionic liquids and their interaction with cellulose. *Chem. Rev.* **2009**, *109*, 6712–6728.
141. Zhu, S.D.; Wu, Y.X.; Chen, Q.M.; Yu, Z.N.; Wang, C.W.; Jin, S.W.; Ding, Y.G.; Wu, G. Dissolution of cellulose with ionic liquids and its application: A mini-review. *Green Chem.* **2006**, *8*, 325–327.
142. Swatloski, R.P.; Spear, S.K.; Holbrey, J.D.; Rogers, R.D. Dissolution of cellulose with ionic liquids. *J. Am. Chem. Soc.* **2002**, *124*, 4974–4975.
143. Li, L.; Meng, L.; Zhang, X.; Fu, C.; Lu, Q. The ionic liquid-associated synthesis of a cellulose/SWCNT complex and its remarkable biocompatibility. *J. Mater. Chem.* **2009**, *19*, 3612–3617.
144. Wan, J.; Yan, X.; Ding, J.J.; Ren, R. A simple method for preparing biocompatible composite of cellulose and carbon nanotubes for the cell sensor. *Sens. Actuators B* **2010**, *146*, 221–225.
145. Zhang, H.; Wang, Z.G.; Zhang, Z.N.; Wu, J.; Zhang, J.; He, H.S. Regenerated-cellulose/multiwalled-carbon-nanotube composite fibers with enhanced mechanical properties prepared with the ionic liquid 1-allyl-3-methylimidazolium chloride. *Adv. Mater.* **2007**, *19*, 698–704.
146. Miyauchi, M.; Miao, J.; Simmons, T.J.; Lee, J.-W.; Doherty, T.V.; Dordick, J.S.; Linhardt, R.J. Conductive cable fibers with insulating surface prepared by coaxial electrospinning of multiwalled nanotubes and cellulose. *Biomacromolecules* **2010**, *11*, 2440–2445.
147. Peng, H.; Meng, L.; Niu, L.; Lu, Q. Simultaneous reduction and surface functionalization of graphene oxide by natural cellulose with the assistance of the ionic liquid. *J. Phys. Chem. C* **2012**, *116*, 16294–16299.

148. Mahmoudian, S.; Wahit, M.U.; Imran, M.; Ismail, A.F.; Balakrishnan, H. A facile approach to prepare regenerated cellulose/graphene nanoplatelets nanocomposite using room-temperature ionic liquid. *J. Nanosci. Nanotechnol.* **2012**, *12*, 5233–5239.
149. Yuan, J.; Antonietti, M. Poly(ionic liquid) latexes prepared by dispersion polymerization of ionic liquid monomers. *Macromolecules* **2011**, *44*, 744–750.
150. Yuan, J.; Antonietti, M. Poly(ionic liquid)s: Polymers expanding classical property profiles. *Polymer* **2011**, *52*, 1469–1482.
151. Green, O.; Grubjesic, S.; Lee, S.; Firestone, M. The design of polymeric ionic liquids for the preparation of functional materials. *Polym. Rev.* **2009**, *49*, 339–360.
152. Mecerreyes, D. Polymeric ionic liquids: Broadening the properties and applications of polyelectrolytes. *Prog. Polym. Sci.* **2011**, *36*, 1629–1648.
153. Fukushima, T.; Kosaka, A.; Yamamoto, Y.; Aimiya, T.; Notazawa, S.; Takigawa, T.; Inabe, T.; Aida, T. Dramatic effect of dispersed carbon nanotubes on the mechanical and electroconductive properties of polymers derived from ionic liquids. *Small* **2006**, *2*, 554–560.
154. Hong, S.H.; Tung, T.T.; Huyen Trang, L.K.; Kim, T.Y.; Suh, K.S. Preparation of single-walled carbon nanotube (SWNT) gel composites using poly(ionic liquids). *Colloid Polym. Sci.* **2010**, *288*, 1013–1018.
155. Xiao, C.H.; Chu, X.C.; Wu, B.H.; Pang, H.L.; Zhang, X.H.; Chen, J.H. Polymerized ionic liquid-wrapped carbon nanotubes: The promising composites for direct electrochemistry and biosensing of redox protein. *Talanta* **2010**, *80*, 1719–1724.
156. Marcilla, R.; Curri, M.L.; Cozzoli, P.D.; Martínez, M.T.; Loinaz, I.; Grande, H.; Pomposo, J.A.; Mecerreyes, D. Nano-objects on a round trip from water to organics in a polymeric ionic liquid vehicle. *Small* **2006**, *2*, 507–512.
157. Meyer, F.; Raquez, J.-M.; Coulembier, O.; de Winter, J.; Gerbaux, P.; Dubois, P. Imidazolium end-functionalized poly(L-lactide) for efficient carbon nanotube dispersion. *Chem. Commun.* **2010**, *46*, 5527–5529.
158. Wu, B.H.; Hu, D.; Kuang, Y.J.; Liu, B.; Zhang, X.H.; Chen, J.H. Functionalization of carbon nanotubes by an ionic-liquid polymer: Dispersion of Pt and PtRu nanoparticles on carbon nanotubes and their electrocatalytic oxidation of methanol. *Angew. Chem. Int. Ed.* **2009**, *48*, 4751–4754.
159. Jia, F.; Shan, C.; Li, F.; Niu, L. Carbon nanotube/gold nanoparticles/polyethylenimine-functionalized ionic liquid thin film composites for glucose biosensing. *Biosens. Bioelectron.* **2008**, *24*, 945–950.
160. Ma, Z.; Yu, J.; Dai, S. Preparation of inorganic materials using ionic liquids. *Adv. Mater.* **2010**, *22*, 261–285.
161. Wildgoose, G.G.; Banks, C.E.; Compton, R.G. Metal nanoparticles and related materials supported on carbon nanotubes: Methods and applications. *Small* **2006**, *2*, 182–193.
162. Kim, T.; Lee, H.; Kim, J.; Suh, K.S. Synthesis of phase transferable graphene sheets using ionic liquid polymers. *ACS Nano* **2010**, *4*, 1612–1618.
163. Kim, T.Y.; Lee, H.W.; Stoller, M.; Dreyer, D.R.; Bielawski, C.W.; Ruoff, R.S.; Suh, K.S. High-performance supercapacitors based on poly(ionic liquid)-modified graphene electrodes. *ACS Nano* **2011**, *5*, 436–442.

164. Zhang, Q.; Wu, S.Y.; Zhang, L.; Lu, J.; Verproot, F.; Liu, Y.; Xing, Z.Q.; Li, J.H.; Song, X.M. Fabrication of polymeric ionic liquid/graphene nanocomposite for glucose oxidase immobilization and direct electrochemistry. *Biosens. Bioelectron.* **2011**, *26*, 2632–2637.
165. Wang, Q.; Yun, Y. Nonenzymatic sensor for hydrogen peroxide based on the electrodeposition of silver nanoparticles on poly(ionic liquid)-stabilized graphene sheets. *Microchim. Acta* **2013**, *180*, 261–268.
166. Zhou, X.S.; Wu, T.B.; Hu, B.J.; Yang, G.Y.; Han, B.X. Synthesis of graphene/polyaniline composite nanosheets mediated by polymerized ionic liquid. *Chem. Commun.* **2010**, *46*, 3663–3665.
167. Tung, T.T.; Kim, T.Y.; Shim, J.P.; Yang, W.S.; Kim, H.; Suh, K.S. Poly(ionic liquid)-stabilized graphene sheets and their hybrid with poly(3,4-ethylenedioxythiophene). *Org. Electron.* **2011**, *12*, 2215–2224.
168. Lonkar, S.P.; Bobenrieth, A.; Winter, J.D.; Gerbaux, P.; Raquez, J.-M.; Dubois, P. A supramolecular approach toward organo-dispersible graphene and its straightforward polymer nanocomposites. *J. Mater. Chem.* **2012**, *22*, 18124–18126.

© 2013 by the authors; licensee MDPI, Basel, Switzerland. This article is an open access article distributed under the terms and conditions of the Creative Commons Attribution license (<http://creativecommons.org/licenses/by/3.0/>).